Nanoscience and Nanotechnology Letters
Vol. 8, 791–797, 2016

Enhancing Efficiency of Silicon Photovoltaic Cells Using High Frequency Electric Pulses

Santosh Kumar[1,*], Naresh C. Sharma[1], and Samar Saha[2]

[1] *Ultrasolar Technology, 1025 Comstock Street, Santa Clara CA 95054, USA*
[2] *Santa Clara University, Santa Clara, California 95053, USA*

This paper presents a method to enhance the efficiency of silicon photovoltaic (Si PV) cells by creating metastable high energy states in the conduction band of silicon with high frequency electric fields and a theoretical model to predict the appearance of the metastable energy states. The states are generated by the interaction of the oscillating electric field from the high frequency electric pulses with the electrostatic potential equilibrium in the lattice. Dramatic increase in the output energy of c-Si PV cells has been observed upon application of extremely high frequency (>50 GHz) electric pulses. Analysis of absorption spectroscopy shows the appearance of multiple additional absorption peaks in visible as well as high energy region (<400 nm) of the solar spectrum. It is concluded that the additional energy generated comes from capturing of hot carriers which are the electrons and holes generated when the PV cell absorbs photons with energy above the bottom of conduction band. These carriers (electrons and holes) lose their energy by the process of thermalization within a few picoseconds. It appears that the interaction of high frequency electric pulses with silicon lattice enables the lattice to delay the thermalization to >200 μs (similar to minority carrier life time) and enables the electrode to capture these hot carriers before the energy is lost by thermalization. Pulses used to generate the states are produced using a special nanostructure involving perovskite based pyroelectric material.

Keywords: Photovoltaics, Hot Carriers, Energy State, High Frequency Pulses, Nanostructure, Pyroelectric.

1. INTRODUCTION

With the widespread adaptation of solar energy as a substitute for the environmentally damaging fossil fuel based energy, the cost of solar energy has significantly come down.[1,2] However in order to further increase the adaptation, without being supported by the government subsidies it is important that new technologies be used to bring the cost of solar energy further down. Attempts are being made to improve the 3rd Generation[3–6] photovoltaic technology (PV) to dramatically improve the energy output of solar cells to bring the cost down. One of the major attempts being made in this area is the development of HCSC (hot carrier solar cells).[6–8]

Hot carriers are the electrons and holes generated upon the absorption of photons with energy above the conduction band of the PV material. For example, in silicon, a photon with wavelength lower than 650 nm (1.9 eV) generates hot carrier upon being absorbed by silicon. These carriers have a lifetime of the order of pico-seconds.[8,9] These carriers are not collected by the PV electrode in their high energy state because approximately 200 μs lifetime is required for the electrode to collect these carriers. These carriers are not stable because no quantum state is available in silicon at those energy levels. Therefore the electrons lose their energy and drop to a more stable state, e.g., the bottom of the conduction band. The energy lost by the electrons in this process is dissipated as heat. The process of losing this energy is called Thermalization.[8,9]

There are several studies on capturing hot-carriers before thermalization occurs.[8] Techniques involving materials and structure optimization are used to capture hot-electrons.[10,11] These methods are expensive and time consuming. Also, interaction of electromagnetic radiation with PV has been well studied in the past.[12–16] However, these studies are inefficient to significantly enhance efficiency of PV cells. Therefore, development of an efficient technique to capture hot-carriers in solar cells as well as an analytical model to predict the effect of capture are utmost important. In this paper, we present the effect of applying multi-frequency electric pulses on entire crystal and a model for the mechanism of hot-carrier capture to enhance PV cell efficiency. The motivation behind this work is to

*Author to whom correspondence should be addressed.

develop a low cost and easily adaptable method which is external to the PV, therefore is useful for existing as well as new PV installations.

Temporary quantum states have been generated in the conduction band which could hold the hot carriers for more than 200 μs. This has been achieved by disturbing the equilibrium of electric potential due to atoms in the lattice using high frequency electric pulses.[24] The correlation between the energy levels of these states and the frequency of the applied pulses has been experimentally demonstrated. A theoretical model of this phenomenon is also developed by modifying the Bloch function and the Hamiltonian operator and using them in the Schrodinger equation to calculate the energy states. It is shown that the model predicts creation of these energy states for certain frequencies only and matches with the experimental data. Finally, we have verified the effectiveness of this approach by

(a) comparing the improvement in the cell energy output with an identical cell without the application of these pulses under different monochromatic ambient illumination;

(b) by analysis of absorbed radiation when the cell is subjected to the pulses.

In this paper we not only present a model but also prove experimentally that the application of high frequency pulses do introduce temporary quantum states supporting the model. We have successfully used this effect to improve the output energy of solar cells.

2. MODEL FOR INTERACTION OF ELECTRIC PULSES WITH SEMICONDUCTOR

Predictions have been made in the past for PV cells performance upon being subjected to electromagnetic radiation. According to Zerbo et al.,[12] the current density as well as recombination velocity can be increased by up to 20% depending upon the energy of the radiation. The frequency used is standard FM radio frequency which is approximately 3 MHz. The mechanism behind this increase is a simple coupling of electric and magnetic fields with the flow of electrons and holes affecting diffusion and drift. Drapalik et al.[15] have predicted $>3\%$ increase in the voltage for cells being subjected to <1 GHz frequencies. The mechanism modeled is the use of demodulated power by the diode behavior of the solar cell. They have demonstrated that Silicon solar cell increases the gain for the frequency it receives through antenna effect with one of the electrodes acting as antenna.

At 50 GHz or higher frequencies, new energy states are created as seen by absorption and photoluminescence spectroscopy. The following paragraphs describe and model a mechanism which appears to be most appropriate based on the experimental findings.

Energy bands are created in a lattice by interaction of electric potentials of the individual atoms or molecules forming the lattice sites. In silicon the bond energy is 2.3 eV. A DC electric field applied to silicon with energy comparable to the bond energy has the potential to impact the electrical potential of the matrix. A high frequency oscillating electric field (pulses) can impact the electric equilibrium and can introduce permissible energy states.

In the following model, we have altered the Bloch potential for the lattice by adding a dynamic potential component from the incoming high frequency electric pulses. We have also used the pulse potential as an operator to alter the Hamiltonian of the lattice as the pulses will alter the way the potentials interact with each other.

The Bloch function for a periodic potential is given by[17]

$$\sum e^{i\boldsymbol{k}\cdot\boldsymbol{r}}\varphi_{\alpha m}C_{\alpha(k)} \tag{1}$$

where $\boldsymbol{k}$ is the wave vector and $\boldsymbol{r}$ is the lattice vector; $\varphi_{\alpha m}$ is the potential between sites α and m; and $C_{\alpha(k)}$ is a constant depending upon α and k.

The time independent Schrodinger Equation for this Bloch function is[18, 19]

$$\sum_{\alpha}\sum_{m} e^{ikr}\langle\varphi_{\alpha o}|H|\varphi_{\alpha m}\rangle C_{\alpha(k)} = E_{c_{\alpha'(k)}} \tag{2}$$

where the Hamiltonian, H is given by

$$H = \frac{-h^2}{2m}\nabla^2 + V(r) \tag{3}$$

Here, $V(r)$ is the static potential at the lattice site (r).

The Hamiltonian in (3) gets impacted by the externally applied pulsed electric field. The extra potential from the high frequency pulses is time dependent and can be expressed as

$$\varphi_u = \varphi_p e^{-i\omega t} \tag{4}$$

where φ_u the additional potential from the applied pulsed electric field; φ_p is the maximum pulse potential; ω is the pulse frequency; and t is the time.

Then the Bloch function can now be expressed as:

$$\sum e^{i\boldsymbol{k}\cdot\boldsymbol{r}}(\varphi_{\alpha m} + \varphi_p e^{-i\omega t})C_{\alpha(k)} \tag{5}$$

It is to be noted that the mass m must be replaced by effective mass μ for time dependent case. Then using

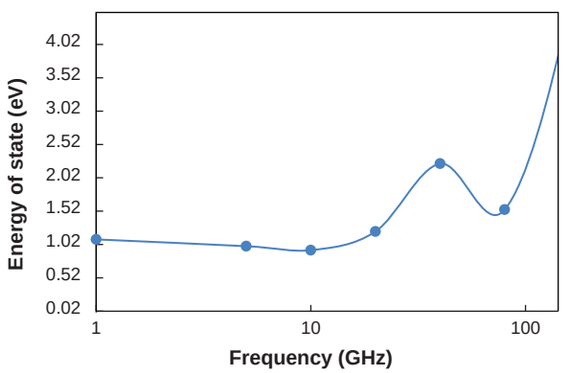

Fig. 1. Energy of states as a function of frequency of applied pulses.

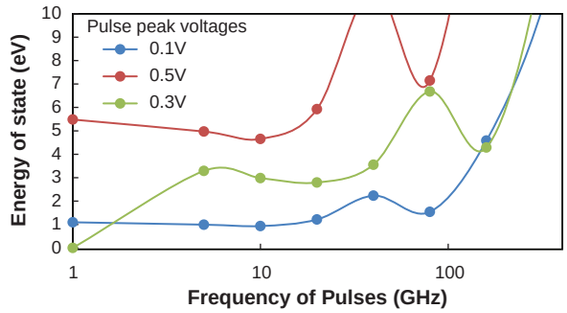

Fig. 2. Dependence of the energy of states upon peak pulse voltages.

4, 5 and 6, the time independent Schrodinger equation now is,

$$\left(\frac{-h^2}{2\mu}\nabla^2 + V(r)\right)\sum e^{i\mathbf{k}\cdot\mathbf{r}}(\varphi_{\alpha m} + \varphi_p e^{-i\omega t})C_{\alpha(k)} = \sum ih\frac{d}{dt}(e^{i\mathbf{k}\cdot\mathbf{r}}\varnothing C_{\alpha(k)}) \quad (6)$$

The energy level can be calculated from the solution of Eq. (6). Expression (7) below is the analytical solution for the energy of the new state(s).

$$\frac{1}{2\mu}\left(\left(\frac{\omega\hbar k^2\varphi_p\cos(kr-\omega\Delta t)}{a} - \hbar k^2\varphi_{\alpha m}\sin(kr)\Delta t\right)^2 + \left\{\begin{array}{c}(\omega\hbar k^2\varphi_p\sin(kr-\omega\Delta t)) + (\hbar\Delta\rho_p\Delta t)\\ +(b\hbar k^2\varphi_{\alpha m}\cos(kr)\Delta t)\end{array}\right\}^2\right)^{1/2} \quad (7)$$

where a and b are constants, $\Delta\rho_p$ is the charge density in the lattice due to the pulses and Δt is the minimum time that the new energy state has to exist in order to increase the power output of the cell. In this analysis, we have used 200 micro-seconds as the value for Δt. Equation (7) relates the creation of metastable states with the applied electric pulses. We have used this equation to predict the generation of new states dependent upon applied frequency of the pulses which has been further experimentally validated.

Figures 1 and 2 are obtained by solving Eq. (7).

In Figure 1, the pulse potential (height) used in the calculation is 100 mV and the charge density is assumed to be 206 C/m^3. Figure 2 shows under the same assumptions, the model prediction for different peak voltages of the pulses. Peak pulse voltage impact the energy of the states as can be intuitively seen. It is clear from the figure that at frequencies above a THz, no energy states are created.

3. EXPERIMENTAL DETAILS

In our experimental setup mono and poly-crystalline silicon solar cells were connected to a high frequency generation device and changes in the cell behavior were observed using (a) *I–V* testing, (b) Absorption spectroscopy and (c) Photoluminescence (PL).

The high frequency pulses were generated using a Fabry-Perot etalon made of nanostructure as shown in Figure 3. The etalon is segmented as shown in Figure 3(A). Figure 3(B) shows a cross section of the nanostructure with 3 layers of pyroelectric films. The refractive indices are chosen such that infrared radiation is trapped in the middle layer. Standing waves in infrared region generate electric charges which are the source of pulses.

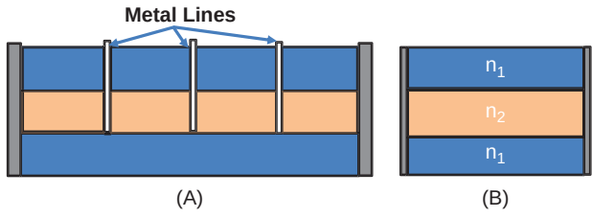

Fig. 3. Segmented etalon nanostructure with pyroelectric films. (A) shows the segments and (B) shows pyroelectric film layers. Refractive index of the top and bottom film is n_1 and refractive index of the middle film is n_2, such than $n_1 > n_2$.

Measurement of the frequency was made using waveguide based frequency meter. The device uses a resonant cavity. The resonant frequency of the cavity is varied by means of a plunger, which is mechanically connected to a micrometer mechanism. Movement of the plunger into the cavity reduces the cavity size and increases the resonant frequency. Conversely, an increase in the size of the cavity (made by withdrawing the plunger) lowers the resonant frequency.[20] High frequency pulses are applied to the solar cell through a cable which essentially works as an antenna. The solar cell is connected to the source of high frequency pulses using this method for about 5 minutes before the experiments are performed.

3.1. *I–V* Measurement

I–V measurements were made on one sample of c-Si solar cell before and after exposure to the pulses. A *Solar Light* Solar Simulator was used at 0.5 Sun intensity for illumination. Keithley current source (2 A max) was used for voltage and current measurements. *I–V* test of the solar cell was carried out in a flash test mode

(i) first without connecting to frequency generating device,

(ii) Second, with frequency generating device connected to the solar cell.

3.2. Absorption Spectroscopy

Ocean Optics USB 2000 portable spectroscope was used for absorption spectroscopy. The experiment was conducted in daylight on a sunny day. The receiver of the spectroscope is approximately 2 mm^2 circular aperture which was focused on a small area of a 125 mm c-Si solar cell. Baseline was initially obtained by analyzing the reflected light from the cell without exposure to the pulses. In the experiment, it was assumed that there is no transmission of the light through the solar cell in the spectrum of interest. The wavelengths analyzed ranged from

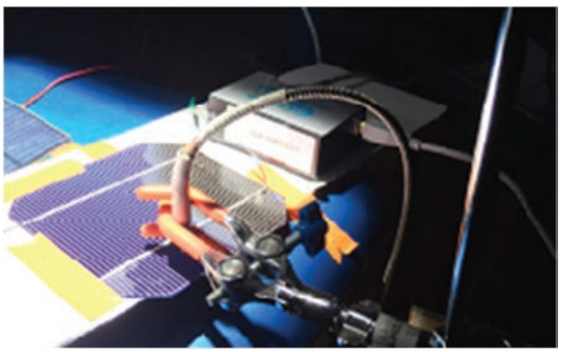

Fig. 4. Picture of the c-Si cell being used with the spectroscope. The box on the right is the spectroscope connected to a computer via USB connection.

200 nm to 1025 nm. Pulses were then applied to the cell by connecting the source of the pulses with a cable to the front of the solar cell which is negative electrode. The reflected light in the same position of the receiver was analyzed. The difference in the two spectrums was calculated. The difference represents the additional absorption in the cell due to the application of pulses.

3.3. Photoluminescence

Ocean Optics USB 2000 portable spectroscope was used operating in differential emission mode to conduct PL test. The test includes subjecting the cell to simulated solar radiation for 30 seconds. After that, the spectroscope was used to detect the emission from the cell in dark condition. Total intensity is calculated by adding the individual intensities at different wavelengths. Next, the pulses were applied to the cell and test was repeated. Cumulative intensities were compared. Figure 4 is the picture of the cell under test along with the spectroscope.

4. RESULTS AND DISCUSSION

4.1. *I–V* Results

Figure 5 shows the *I–V* curve. Brown curves in the figure is obtained by applying the pulses to the cell and the blue curve is the baseline curve without the pulses.

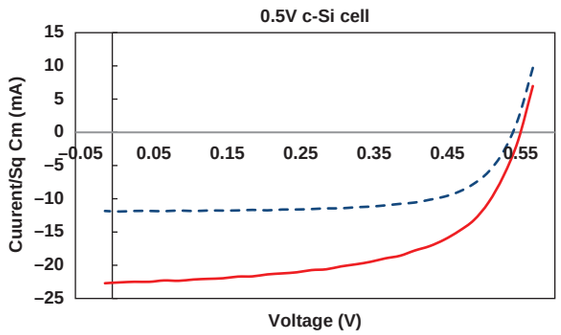

Fig. 5. *I–V* curves with and without pulses. Solid line: with pulses, dashed line: without pulses.

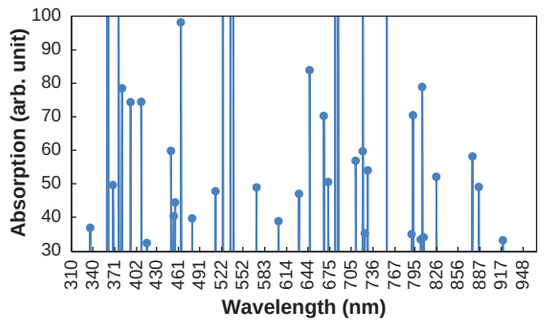

Fig. 6. Additional absorption peaks appear on application of the pulses.

From the analysis of *I–V* data, it is observed that the short circuit current I_{sc} increases upon application of pulses. There is also a minor increase in open circuit voltage V_{oc}. This can be interpreted as increase in the number of carriers available as well as increase in the energy of the carriers upon application of the pulses. Increase in V_{oc} implies higher energy states in the conduction band.

4.2. Absorption Spectroscopy

Figure 6 demonstrates the generation of additional absorption peaks when the solar cell is subjected to the pulses. Sign of the intensity in Figure 6 has been reversed to represent absorption. The observed absorption peaks support the prediction of Figure 1. The data obtained is for frequency range of 50 to 100 GHz. For higher frequencies, it is expected that the absorption peaks will be lower.

The appearance of additional absorption peaks in the spectroscopic analysis clearly demonstrates creation of new energy states upon application of the pulses. Most of the absorption peaks occur at 370 nm, 460 nm, 500 nm and some higher wavelengths.

4.3. Photoluminescence

Figure 7 shows the PL emission from a c-Si cell before and after being subjected to the pulses. Increase in cumulative intensity implies more radiative recombination. Generally radiative recombination is from band to band transition which in the case of silicon PV should be at approximately 1100 nm. In our Photoluminescence analysis we

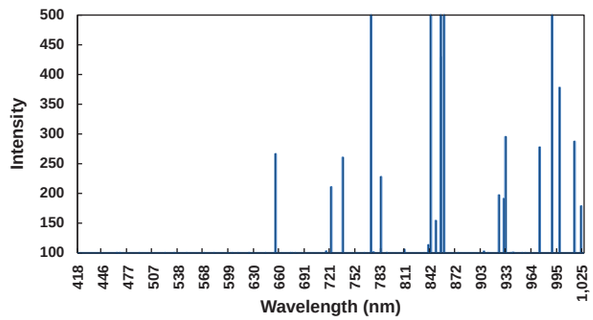

Fig. 7. Additional PL intensities with the pulses for 30 seconds.

discovered that a significant portion of the radiative recombination is from approximately 740 nm (1.68 eV), 920 nm (1.44 eV) and 1000 nm (1.25 eV).

5. ANALYSIS

According to Drapalik et al., a sharp increase in the antenna gain (dB) is seen at 100 MHz in c-Si. However around 1 GHz, there is a drop. From the diode and resistor analysis (simulating the solar cell) of the signal at 100 MHz, at the optimum load, a voltage gain of approximately 3% is predicted. This is an interesting analysis, however it does not discuss the effect at higher frequencies. Other analysis directly couples the electric and magnetic field to the moving electrons in the solar cell and does not discuss high frequency effects.[12]

Interaction of electromagnetic wave with multistate atoms has been studied for a long time.[22, 25] The effect presented in this paper can also be treated as Jaynes-Cumming interaction[25] (quantized electromagnetic wave interacting with a multi-state atom) integrated over the lattice. The Jaynes-Cummings Hamiltonian is given by

$$\hat{H} = -\frac{\hbar\omega_0}{2}\sigma_z + \hbar\omega\hat{a}^\dagger\hat{a} + g(\hat{a}\sigma_+ + \hat{a}^\dagger\sigma_-)$$

ω represents the frequency of the photon and ω_0 is the resonance frequency. The Hamiltonian is for creating an excited state by absorbing a photon and de-exciting a state by creating a photon. Using the electric field oscillation of the pulses to replace the electric field of the photon creation of new excited states can be predicted and calculated using Jaynes-Cummings Hamiltonian. However we have not used this method for calculation and prediction in this paper.

In our experiments, it is consistently observed that additional energy states, generally at much higher level than the bottom of the conduction band appear and participate in the photovoltaic process. Figures 1 and 2 show significantly higher than 3% (as predicted by Drapalik et al.) increase in energy at much higher frequencies. In addition, a much larger increase in both open circuit voltage and short circuit current under blue illumination proves (data not presented here) that with the high frequency pulses, absorption occurs at higher energy levels. These energy states (~2 eV) do not normally exist in silicon and therefore are created. It is not likely that the effect is created by any other mechanisms such as those mentioned in Refs. [13, 15].

From the absorption spectroscopy data, it can be clearly seen than additional states are created at high energy levels.

Figure 9 represents the mechanism of power improvement from pulses. Additional states or 'mini bands' are created due to the pulses. These states are temporary and disappear upon the removal of pulses. From the measurement data, we have found these states to be metastable

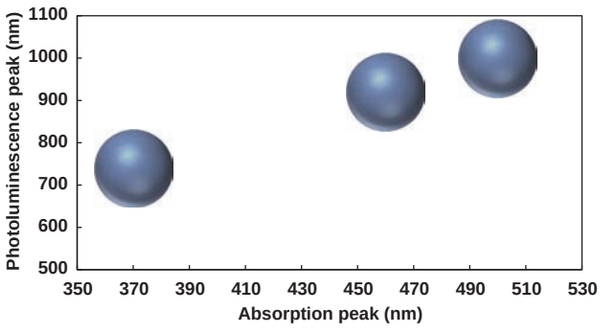

Fig. 8. Graph of absorption peak versus photoluminescence peak.

with a lifetime comparable to the minority carrier life time of the cell (silicon). When a hot carrier is generated upon the absorption of high energy photon, the hot carriers occupy the newly generated metastable states and therefore do not thermalize in picoseconds. These carriers contribute to the energy output of the cell.

5.1. Increased Voltage versus Increased Current

It is generally believed that capturing the energy of hot carries would increase PV open circuit voltage and not the short circuit current. The reason for increased open circuit voltage is that hot carriers lose their energy only by dropping to the bottom of conduction band. Since they are still in the conduction band, they are available to contribute to current. By preventing the loss of energy, the carrier's potential energy becomes available which increases the open circuit voltage.

In our experiments however, both voltage and current increases have been observed. The voltage increase can be explained by the conventional understanding of hot carriers. Current increase is possible with multi-exciton generation. [21, 23] Additional data which supports the generation of multi-exciton in our experiments is from the photoluminescence measurements. It can be observed from comparison of the absorption peaks in Figure 6 with the PL peaks in Figure 7 that the wavelengths of absorption peaks approximately correspond to half the wavelength of the PL peaks, suggesting that the energies of the photons

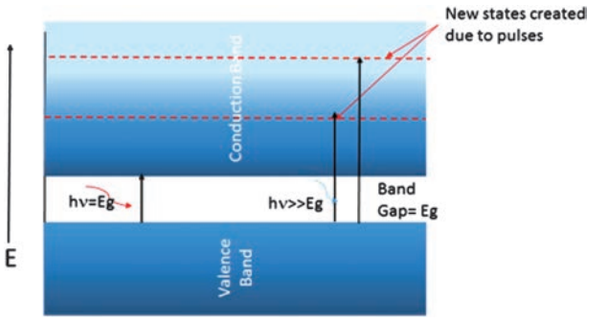

Fig. 9. Simplified energy band diagram showing quantum states.

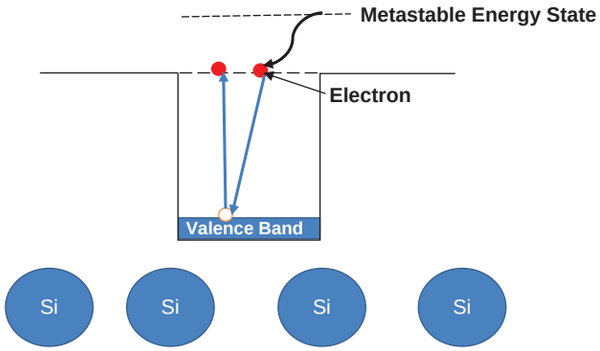

Fig. 10. Quantum well created by pulse potential.

absorbed is approximately 2× the energy of photons emitted in PL. This relationship can be very clearly seen from Figure 8. This condition occurs when absorption of one photon results in generation of 2 excitons, each with half the energy of the absorbed photon.

According to generally accepted theory, for multi exciton to occur, coulombic attraction between a hot electron and a valence band hole is required.[23] This mechanism is more likely to occur in a nanostructure due to quantum confinement. Quantum confinement enhances the coulombic interaction between electron and hole.

Figure 10 depicts the creation of quantum well by the pulses. It is likely that the pulses may cause quantum confinement necessary for multi-exciton generation to occur. For the quantum confinement to occur, the potential inside the potential well has to be zero. This can happen when the pulses are forming a standing potential wave with an effective potential at a point which is of opposite polarity and same magnitude as compared to the potential at that point due to coulombic interaction between lattice sites. Figure 11 depicts qualitatively a scenario which would allow the quantum confinement to occur.

Under these condition it is feasible to create a multi exciton scenario.

Time resolved absorption spectroscopy has not been done yet for further confirmation of multi excitons.

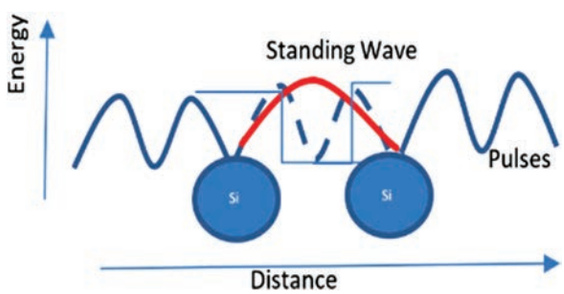

Fig. 11. Qualitative depiction of a scenario that could create quantum confinement similar to nanostructure. The *Y* axis is the electrostatic potential energy.

6. CONCLUSION

The method discussed in this paper has been demonstrated to create metastable energy states in silicon solar cells. We have discussed the theory behind it and proven that theory permits the creation of these states. Results included in this paper show direct verification of creation of these states by absorption spectroscopy. It has also been theorized that creation of quantum wells is possible which may cause multi-excitons to occur and explain the increase in current. The authors have demonstrated in the past that a significant increase in voltage and current can be obtained by applying high voltage MHz pulses on the solar cells.[24] The method has further been applied on larger scale by the authors for improvement of total harvested energy at actual solar installations.

References and Notes

1. I. D. Feldman, G. Barbose, R. Margolis, T. James, S. Weaver, N. Darghouth, R. Fu, C. Davidson, and R. Wiser, Photovoltaic System Pricing Trends: Historical, Recent, and Near-Term Projections, 2014 edn., US Department of Energy, NREL/PR-6A20-62558 **(2014)**.
2. R. Ze'ev, M. G. Abrams, N. Avi, G. Chris, and Z. Xiang, *Sol. Energy Mater. Sol. Cells* 99, 308 **(2012)**.
3. M. Bernardi, D. Vigil-Fowler, J. Lischner, J. B. Neaton, and S. G. Louie, *Phys. Rev. Lett.* 112, 257402 **(2014)**.
4. M. A. Green, C. Gavin, K. Dirk, S. Shrestha, H. Shujuan, A. Pasquale, and T. Lara, Hot carrier solar cells: Challenges and recent progress, *2010 IEEE 35th Photovoltaic Specialists Conference (PVSC)*, Honolulu, Hawai **(2010)**, pp. 57–60.
5. P. Aliberti, Y. Feng, Y. Takeda, S. K. Shrestha, M. A. Green, and G. Conibeer, *J. Appl. Phys.* 108, 094507 **(2010)**.
6. N. J. Ekins-Daukes, Routes to high efficiency photovoltaic power conversion, *2013 IEEE 39th Photovoltaic Specialists Conference (PVSC)*, Tampa, Florida **(2013)**, pp. 0013–0016.
7. J. Rodière, L. J.-F. Lombez, H. F. Guillemoles, and D. Olivier, InP/InGaAsP heterostructures for hot carrier solar cells (HCSC), *28th European Photovoltaic Solar Energy Conference (EU PVSEC 2013)*, Paris, France **(2013)**, pp. 127–128.
8. A. Le Bris and J.-F. Guillemoles, *Appl. Phys. Lett.* 97, 113506 **(2010)**.
9. P. Maurizia, M. Bernardi, and J. C. Grossman, *Nano Lett.* 15, 2794 **(2015)**.
10. D. Sangalli and A. Marini, *Europhys. Lett.* 110, 47004 **(2015)**.
11. S. Erel, *Sol. Energy Mater. Sol. Cells* 71, 273 **(2002)**.
12. I. Zerbo, M. Zoungrana, A. Ouedraogo, B. Korgo, B. Zouma, and D. J. Bathiebo, *Global J. Pure Appl. Sci.* 20, 139 **(2014)**.
13. M. Sane, *Indian J. Pure Appl. Phys.* 53, 590 **(2015)**.
14. M. Drapalik, J. Schmid, E. Kancsar, V. Schlosser, and G. Klinger, A study of the antenna effect of photovoltaic modules, *Proceedings of the International Conference on Renewable Energies and Power Quality (ICREPQ)*, Granada, Spain, March **(2010)**, pp. 23–25.
15. T. Wada, T. Tomiyuki, M. Mori, T. Masamitsu, S. Shoichi, and I. Hironobu, Radiated electromagnetic field from a solar cell for CISPR radiated emission measurement method, *IEEE 2005 International Symposium on Electromagnetic Compatibility (EMC 2005)*, Chicago, Illinois **(2005)**, Vol. 1, pp. 112–117.
16. D. Piazza, M. Carmela, C. Serporta, G. Tine, and G. Vitale, Electromagnetic compatibility characterization of the DC side in a low power photovoltaic plant, *Industrial Technology, 2004 IEEE International Conference (ICIT 04)* **(2004)**, Vol. 2, pp. 672–677.
17. C. Kittel, Introduction to Solid State, John Wiley & Sons, Hoboken, NJ **(1966)**.

18. D. R. Hofstadter, *Physical Review B* 14, 2239 (**1976**).
19. J. H. Shirley, *Physical Review* 138, B979 (**1965**).
20. A. Nassiri, Microwave Physics and Techniques, USPAS, Santa Barbara, June (**2003**).
21. H. Hirori, K. Shinokita, M. Shirai, S. Tani, Y. Kadoya, and K. Tanaka, *Nature Communications* 2, 594 (**2011**).
22. I. Rabi, *Physical Review* 51, 652 (**1937**).
23. R. D. Schaller and V. I. Klimov, *Phys. Rev. Lett.* 92, 186601 (**2004**).
24. S. Kumar, N. C. Sharma, B. R. Mehta, and S. K. Saha, A novel low-cost pyroelectric device for enhancing the efficiency of solar cell, *Proceedings of International Conference on Green Energy and Technology (ICGET'13)*, Kitakyushu, Japan, August (**2013**), pp. 181–184.
25. E. T. Jaynes and F. W. Cummings, *Proc. IEEE* 51, 89 (**1963**).

Received: 12 September 2016. Accepted: 19 September 2016.